



Centrum voor Wiskunde en Informatica

**REPORT***RAPPORT*

*MAS*

*Modelling, Analysis and Simulation*



*Modelling, Analysis and Simulation*

The Hamiltonian Particle-Mesh Method for the Spherical  
Shallow Water Equations

Jason Frank, Sebastian Reich

**REPORT MAS-E0317 DECEMBER 8, 2003**

CWI is the National Research Institute for Mathematics and Computer Science. It is sponsored by the Netherlands Organization for Scientific Research (NWO).

CWI is a founding member of ERCIM, the European Research Consortium for Informatics and Mathematics.

CWI's research has a theme-oriented structure and is grouped into four clusters. Listed below are the names of the clusters and in parentheses their acronyms.

Probability, Networks and Algorithms (PNA)

Software Engineering (SEN)

**Modelling, Analysis and Simulation (MAS)**

Information Systems (INS)

Copyright © 2003, Stichting Centrum voor Wiskunde en Informatica

P.O. Box 94079, 1090 GB Amsterdam (NL)

Kruislaan 413, 1098 SJ Amsterdam (NL)

Telephone +31 20 592 9333

Telefax +31 20 592 4199

ISSN 1386-3703

# The Hamiltonian Particle-Mesh Method for the Spherical Shallow Water Equations

## ABSTRACT

The Hamiltonian particle-mesh (HPM) method is generalized to the spherical shallow water equations, utilizing constrained particle dynamics on the sphere and smoothing with Merilees' double-periodic FFT formulation of  $\mathcal{O}(J^2 \log J)$  in the latitudinal gridsize. The time step for the explicit, symplectic integrator depends only on the uniform smoothing length.

*2000 Mathematics Subject Classification:* 65M99, 86A10

*Keywords and Phrases:* shallow water equations, spherical geometry, particle-mesh method, Hamiltonian equations of motion, constraints, symplectic integration

*Note:* Work of J. Frank is carried out under project MAS1.3 - 'Numerical Analysis of PDEs.' Funding from an NWO Innovative Research Grant is gratefully acknowledged. S. Reich acknowledges partial financial support by EPSRC Grant GR/R09565/01.

# The Hamiltonian Particle-Mesh Method for the Spherical Shallow Water Equations

Jason Frank

CWI

*P.O. Box 94079, 1090 GB Amsterdam, The Netherlands*

Sebastian Reich

*Department of Mathematics, Imperial College of London*

*180 Queen's Gate, London, SW7 2AZ, England*

## ABSTRACT

The Hamiltonian particle-mesh (HPM) method is generalized to the spherical shallow water equations, utilizing constrained particle dynamics on the sphere and smoothing with Merilees' double-periodic FFT formulation of  $\mathcal{O}(J^2 \log J)$  in the latitudinal gridsize. The time step for the explicit, symplectic integrator depends only on the uniform smoothing length.

*2000 Mathematics Subject Classification:* 65L06, 65xxx

*Keywords and Phrases:* shallow water equations, spherical geometry, particle-mesh method, Hamiltonian equations of motion, constraints, symplectic integration

*Note:* Work of J. Frank is carried out under project MAS1.3 - 'Numerical Analysis of PDEs.' Funding from an NWO Innovative Research Grant is gratefully acknowledged. S. Reich acknowledges partial financial support by EPSRC Grant GR/R09565/01.

## 1. INTRODUCTION

Spherical harmonic and gridpoint discretizations of geophysical fluids on the sphere encounter strict limitations on maximum stable time stepsize for explicit integrators, due to the CFL condition near the poles. Semi-Lagrangian methods largely avoid these restrictions, but only by giving up strict conservation of mass and energy. By working with a fully Lagrangian description, and embedding the sphere in  $\mathbb{R}^3$ , one can avoid pole-related stepsize limitations and retain exact conservation of mass, energy and circulation. Additionally, the method can be made symplectic, which has even stronger implications, and in particular implies conservation of potential vorticity.

In this paper, we extend the Hamiltonian particle-mesh (HPM) method of FRANK, GOTTWALD & REICH [6, 5] to the shallow water equations in spherical geometry [11]. We take CÔTE's [2] three-dimensional constrained formulation

$$\begin{aligned}\frac{d}{dt}\mathbf{x} &= \mathbf{v}, \\ \frac{d}{dt}\mathbf{v} &= -2\Omega\mathbf{k} \times \mathbf{v} - g\nabla_{\mathbf{x}}h - \lambda\mathbf{x}, \\ 0 &= \mathbf{x} \cdot \mathbf{x} - R^2\end{aligned}$$

as a starting point to derive an approximation to the shallow water equations in the form of a constrained system of ordinary differential equations (ODEs) in the particle positions  $\mathbf{x}_k$  and their velocities  $\mathbf{v}_k$ ,  $k = 1, \dots, K$ . Here  $g = 9.80616 \text{ m s}^{-2}$  is the gravitational constant,  $\Omega = 7.292 \times 10^{-5} \text{ s}^{-1}$  is

the rotation rate of the earth,  $R = 6.37122 \times 10^6$  m is the radius of the earth,  $h$  is the geopotential layer depth,  $\mathbf{k} = (0, 0, 1)^T$ , and  $\lambda$  is a Lagrange multiplier to enforce the position constraint.

A key aspect of the HPM method is the smoothing or regularization of the particle-based discrete mass distribution over a computational grid, which yields the layer depth. To implement this idea in the setting of the present paper we utilize a spherical FFT method first suggested by MERILEES [9]. MERILEES' method requires  $\mathcal{O}(J^2 \log J)$  operations per smoothing step contrary to  $\mathcal{O}(J^3)$  operations necessary for the spectral transform method [10]. Here  $J$  denotes the number of grid points in the latitudinal direction. We note that for very fine discretizations, or in a parallel computing environment, the FFT-based smoother may be replaced by a gridpoint based approximation without significantly influencing our results.

Another key aspect of the HPM method lies in the variational or Hamiltonian nature of the spatial truncation. This property combined with a symplectic time-stepping algorithm [7] guarantees excellent conservation of total energy and circulation [5]. These desirable properties also apply to the proposed HPM in spherical geometry and we demonstrate this for a numerical test problem from [11]. Finally, the time steps achievable for our semi-explicit symplectic integration method are entirely determined by the uniform smoothing length and not by the longitude-latitude grid size near the poles.

## 2. DESCRIPTION OF THE SPATIAL TRUNCATION

The *Hamiltonian particle-mesh* (HPM) method utilizes a set of  $K$  particles with coordinates  $\mathbf{x}_k \in \mathbb{R}^3$  and velocities  $\mathbf{v}_k \in \mathbb{R}^3$  as well as a *longitude-latitude grid* with equal grid spacing  $\Delta\lambda = \Delta\theta = \pi/J$ . The latitude grid points are offset a half-grid length from the poles. Hence we obtain grid points  $(\lambda_m, \theta_n)$ , where  $\lambda_m = m\Delta\lambda$ ,  $\theta_n = -\frac{\pi}{2} + (n - 1/2)\Delta\theta$ ,  $m = 1, \dots, 2J$ ,  $n = 1, \dots, J$ , and the grid dimension is  $2J \times J$ .

All particle positions satisfy the holonomic constraint

$$\mathbf{x}_k \cdot \mathbf{x}_k = R^2, \quad (2.1)$$

where  $R > 0$  is the radius of the sphere. Differentiating the constraint (2.1) with respect to time immediately implies the velocity constraint

$$\mathbf{x}_k \cdot \mathbf{v}_k = 0. \quad (2.2)$$

We convert between *Cartesian* and *spherical coordinates* using the formulas

$$x = R \cos \lambda \cos \theta, \quad y = R \sin \lambda \cos \theta, \quad z = R \sin \theta,$$

and

$$\lambda = \tan^{-1} \left( \frac{y}{x} \right), \quad \theta = \sin^{-1} \left( \frac{z}{R} \right).$$

Hence we associate with each particle position  $\mathbf{x}_k = (x_k, y_k, z_k)^T$  a spherical coordinate  $(\lambda_k, \theta_k)$ .

The implementation of the HPM method is greatly simplified by making use of the *periodicity* of the spherical coordinate system in the following sense. The periodicity is trivial in the longitudinal direction. For the latitude, a great circle meridian is formed by connecting the latitude data separated by an angular distance  $\pi$  in longitude (or  $J$  grid points). See, for example, the paper by SPOTZ, TAYLOR & SWARZTRAUBER [10].

Let  $\psi^{mn}(\mathbf{x})$  denote the *tensor product cubic B-spline* centered at a grid point  $(\lambda_m, \theta_n)$ , i.e.

$$\psi^{mn}(\mathbf{x}) \equiv \psi_{\text{cs}} \left( \frac{\lambda - \lambda_m}{\Delta\lambda} \right) \cdot \psi_{\text{cs}} \left( \frac{\theta - \theta_n}{\Delta\theta} \right), \quad (2.3)$$

where  $\psi_{\text{cs}}(r)$  is the cubic spline

$$\psi_{\text{cs}}(r) \equiv \begin{cases} \frac{2}{3} - |r|^2 + \frac{1}{2}|r|^3, & |r| \leq 1, \\ \frac{1}{6}(2 - |r|)^3, & 1 < |r| \leq 2, \\ 0, & |r| > 2 \end{cases}$$

and  $(\lambda, \theta)$  are the spherical coordinates of a point  $\mathbf{x}$  on the sphere.

In evaluating (2.3) it is understood that the distances  $\lambda - \lambda_m$  and  $\theta - \theta_n$  are taken as the minimum over all periodic images of the arguments. With this convention the basis functions form a *partition of unity*, i.e.

$$\sum_{m,n} \psi^{mn}(\mathbf{x}) = 1, \quad (2.4)$$

hence satisfying a minimum requirement for approximation from the grid to the rest of the sphere.

The gradient of  $\psi^{mn}(\mathbf{x})$  in  $\mathbb{R}^3$  can be computed using the chain rule and the standard formula

$$\nabla_{\mathbf{x}} = \frac{1}{R} \hat{\boldsymbol{\theta}} \frac{\partial}{\partial \theta} + \frac{1}{R \cos \theta} \hat{\boldsymbol{\lambda}} \frac{\partial}{\partial \lambda}$$

with unit vectors

$$\hat{\boldsymbol{\theta}} = \begin{bmatrix} -\cos \lambda \sin \theta \\ -\sin \lambda \sin \theta \\ \cos \theta \end{bmatrix}, \quad \hat{\boldsymbol{\lambda}} = \begin{bmatrix} -\sin \lambda \\ \cos \lambda \\ 0 \end{bmatrix}.$$

Let us assume for a moment that we have computed a layer depth approximation  $\hat{H}_{mn}(t)$  over the longitude-latitude grid. Making use of the partition of unity (2.4), a continuous layer depth approximation is obtained

$$\hat{h}(\mathbf{x}, t) = \sum_{mn} \hat{H}_{mn} \psi^{mn}(\mathbf{x}). \quad (2.5)$$

Computing the gradient of this approximation at particle positions  $\mathbf{x}_k$ , the Newtonian equations of motion for each particle on the sphere are given by the constrained formulation

$$\frac{d}{dt} \mathbf{x}_k = \mathbf{v}_k, \quad (2.6)$$

$$\frac{d}{dt} \mathbf{v}_k = -2\Omega \mathbf{k} \times \mathbf{v}_k - g \sum_{m,n} \nabla_{\mathbf{x}_k} \psi^{mn}(\mathbf{x}_k) \hat{H}_{mn}(t) - \lambda_k \mathbf{x}_k, \quad (2.7)$$

$$0 = \mathbf{x}_k \cdot \mathbf{x}_k - R^2. \quad (2.8)$$

To close the equations of motion, we define the geopotential layer depth  $\hat{H}_{mn}(t)$  as follows. We assign to each particle a fixed mass  $m_k$  which represents its local contribution to the layer depth approximation. Let us assume that the particles are essentially equidistributed over the sphere at the initial time  $t = 0$ . First, we compute

$$A_{mn} = \sum_k \psi^{mn}(\mathbf{x}_k). \quad (2.9)$$

We find that  $A_{mn}$  is not approximately constant but rather

$$A_{mn} \approx \cos(\theta_m) \cdot \text{const},$$

i.e.,  $A_{mn}$  is proportional to the area of the associated longitude-latitude grid cell on the sphere. Second, we define the particle masses

$$m_k = \sum_{m,n} H_{mn} \psi^{mn}(\mathbf{x}_k), \quad (2.10)$$

and obtain

$$H_{mn} \approx \frac{1}{A_{mn}} \sum_k m_k \psi^{mn}(\mathbf{x}_k),$$

which provides us with the desired layer depth approximation. The area coefficients (2.9) and the particle masses (2.10) are only computed once at the beginning of the simulation. During the simulation the layer depth is approximated over the longitude-latitude grid using the formula

$$H_{mn}(t) = \frac{1}{A_{mn}} \sum_k m_k \psi^{mn}(\mathbf{x}_k(t)). \quad (2.11)$$

A crucial step in the development of an HPM method is the implementation of an appropriate smoothing operator  $\mathbf{S}$  over the longitude-latitude grid. We will derive such a smoothing operator in the subsequent section. For now we simply assume the existence of a symmetric linear operator  $\mathbf{S}$  and define smoothed grid functions via  $\mathbf{S} : \{A_{mn}\} \rightarrow \{\tilde{A}_{mn}\}$  and  $\mathbf{S} : \{M_{mn}\} \rightarrow \{\tilde{M}_{mn}\}$ , respectively, where

$$M_{mn}(t) = \sum_k m_k \psi^{mn}(\mathbf{x}_k(t)).$$

We now replace the definition (2.11) by

$$\tilde{H}_{mn}(t) = \frac{\tilde{M}_{mn}(t)}{\tilde{A}_{mn}} \quad (2.12)$$

and finally introduce  $\hat{H}_{mn}(t)$  via  $\mathbf{S} : \{\tilde{H}_{mn}\} \rightarrow \{\hat{H}_{mn}\}$ . This approximation is used in (2.7) and closes the equations of motion.

### Conservation properties.

The HPM method conserves mass, energy, symplectic structure, circulation, potential vorticity, and geostrophic and hydrostatic balances:

Trivially, since the *mass* associated with each particle is fixed for the entire integration, the HPM method has local and total mass conservation. Furthermore, (2.4) implies  $\frac{d}{dt} \sum_{m,n} M_{m,n} = 0$ , and the same will hold for  $\tilde{M}_{mn}(t)$  for appropriate  $\mathbf{S}$ . This implies the conservation of  $\sum_{mn} \tilde{H}_{mn}(t) \tilde{A}_{mn}$  by (2.12).

*Circulation* is also conserved in the following sense. Since by (2.7) the particles are accelerated in the exact gradient field of the continuous layer depth approximation (2.5), the discrete particle flow may be embedded in a continuum particle flow that satisfies a circulation theorem. See [5] for a full discussion.

The equations of motion (2.6)–(2.8) define a constrained Hamiltonian system that conserves the *total energy* (Hamiltonian)

$$\mathcal{H} = \sum_k \frac{m_k}{2} \mathbf{v}_k \cdot \mathbf{v}_k + \frac{g}{2} \sum_{m,n} \tilde{H}_{mn}^2 \tilde{A}_{mn}.$$

Note that  $\tilde{H}_{mn}^2 \tilde{A}_{mn} = \tilde{M}_{mn}^2 \tilde{A}_{mn}^{-1}$ . The *symplectic structure* of phase space is given by

$$\omega = \sum_k m_k d\mathbf{v}_k \wedge \mathbf{x}_k + \Omega \sum_k m_k d\mathbf{x}_k \wedge (\mathbf{k} \times d\mathbf{x}_k). \quad (2.13)$$

The symplectic structure may be also be embedded in a continuum particle flow which allows one to pull back to label space by writing the particle flow as a function of the initial conditions. One consequence of this is a statement of *potential vorticity* conservation. See [1] for a complete account.

See also [3] for a discussion of the preservation properties of HPM for *adiabatic invariants* such as the geostrophic and hydrostatic balance relations.

### 3. THE SMOOTHING OPERATOR

To complete the description of the HPM method, we need to find an inexpensive smoothing operator that averages out fluctuations over the sphere on a length scale shorter than  $\Lambda$ . Following MERILEES' pseudospectral code [9], we employ one-dimensional fast Fourier transforms (FFTs) along the longitudinal and the latitudinal directions as summarized, for example, by FORNBERG [4] and SPOTZ, TAYLOR & SWARZTRAUBER [10]. This allows us to essentially follow the HPM smoothing approach of FRANK, GOTTFELD & REICH [6, 5], which achieves smoothing by inverting a modified Helmholtz operator. In particular, one can easily solve modified Helmholtz equations separately in the longitudinal and latitudinal directions and apply an operator splitting idea to define a two-dimensional smoothing operator.

We use the following technique to achieve uniform smoothing over the sphere with a smoothing length  $\Lambda$ . In the lateral direction we use the modified Helmholtz operator

$$\mathbb{H}_{\text{lat}}(\Lambda^2) = 1 - \frac{\Lambda^2}{R^2} \frac{\partial^2}{\partial \theta^2}.$$

The longitudinal direction is slightly more complicated because one has to compensate for the varying length of the associated circles on the sphere. The natural choice is

$$\mathbb{H}_{\text{lon}}(\Lambda^2) = 1 - \frac{\Lambda^2}{R^2 \cos^2 \theta} \frac{\partial^2}{\partial \lambda^2}$$

and, using a second order operator splitting, the complete smoothing operator can schematically be written as

$$\mathbb{S} = \mathbb{H}_{\text{lon}}^{-1}(\Lambda^2/2) \circ \mathbb{H}_{\text{lat}}^{-1}(\Lambda^2) \circ \mathbb{H}_{\text{lon}}^{-1}(\Lambda^2/2).$$

Upon implementing these operators using FFTs, we obtain a discrete approximation  $\mathbf{S}$  over the longitude-latitude grid which was used in the previous section to define the layer depth  $\hat{H}_{mn}$ .

### 4. TIME DISCRETIZATION AND NUMERICAL EXPERIMENTS

Since the equations of motion (2.6)–(2.8) are Hamiltonian, it is desirable to integrate them with a symplectic method, as this implies long-time approximate conservation of energy, symplectic structure (and hence PV) and adiabatic invariants such as geostrophic balance. Therefore, the following



modification of the symplectic RATTLE/SHAKE algorithm [7] suggests itself:

$$\begin{aligned}
\mathbf{v}_k^{n+1/2} &= (\mathbf{I} + \Delta t \Omega \mathbf{k} \times)^{-1} \left[ \mathbf{v}_k^n - \frac{g \Delta t}{2} \nabla_{\mathbf{x}_k} \sum_{m,n} \psi^{mn}(\mathbf{x}_k^n) \hat{H}_{mn}(t_n) - \lambda_k^n \mathbf{x}_k^n \right], \\
\mathbf{x}_k^{n+1} &= \mathbf{x}_k^n + \Delta t \mathbf{v}_k^{n+1/2}, \\
0 &= \mathbf{x}_k^{n+1} \cdot \mathbf{x}_k^{n+1} - R^2, \\
\bar{\mathbf{v}}_k^{n+1} &= (\mathbf{I} - \Delta t \Omega \mathbf{k} \times) \mathbf{v}_k^{n+1/2} - \frac{g \Delta t}{2} \nabla_{\mathbf{x}_k} \sum_{m,n} \psi^{mn}(\mathbf{x}_k^{n+1}) \hat{H}_{mn}(t_{n+1}), \\
\mathbf{v}_k^{n+1} &= \bar{\mathbf{v}}_k^{n+1} - R^{-2} \mathbf{x}_k (\mathbf{x}_k^{n+1} \cdot \bar{\mathbf{v}}_k^{n+1}).
\end{aligned}$$

The first three equations, solved simultaneously, lead to a scalar quadratic equation in the Lagrange multiplier  $\lambda_k^n$  for each  $k$ . The roots correspond to projecting the particle to the near and far sides of the sphere, so the smallest root is taken. The last two equations update the velocity field and enforce (2.2). Hence the above time stepping method is explicit. One can show that the method also conserves the symplectic two form (2.13) and hence is symplectic [7].

To validate the HPM method, we integrated Test Case 7 (Analyzed 500 mb Height and Wind Field Initial Conditions) from WILLIAMSON, DRAKE, HACK, JAKOB & SWARZTRAUBER [11] with the initial data of 21 December 1978 (T213 truncation), over an interval of 5 days. All calculations were done in Matlab, using *mex* extensions in C for particle-mesh operators. See also results reported electronically at <http://www.cwi.nl/projects/gi/HPM/>.

The discretization parameters (number of latitudinal gridpoints  $J$ , total number of particles  $K$ , smoothing length  $\Lambda$ , and time stepsize of  $\Delta t$ ) for the various runs are listed in the table below:

$J$	$K$	$\Lambda$ (m)	$\Delta t$ (s)
128	333758	$3.1275 \times 10^5$	1728
256	1335096	$1.5637 \times 10^5$	864
384	3003976	$1.0425 \times 10^5$	432

A stereographic projection of the geopotential field in the northern hemisphere is shown in Figure 1 for the  $J = 384$  simulation, and agrees quite well with the solution shown in Figure 5.13 of [8]. In Figure 2 we give a comparison of the solutions obtained for  $J = 128$ ,  $J = 256$ , and  $J = 384$  with the T213 reference solution. The error in the geopotential fields for these same cases is compared in Figure 3. The reader will note that there is an error in the geopotential at time  $t = 0$  already. This error is due to the fact that the geopotential is determined by the particle masses  $m_k$ . The mass coefficients are assigned initially with a certain approximation error.

Figure 4 shows the growth of error in the  $\ell_2$ -norm for the geopotential height over the 5 day period, for  $J = 128$ ,  $J = 256$  and  $J = 384$ . We observe approximately first order convergence. (A numerical approximation of the order exponent based on the given data gave  $p \approx 1.3$ .)

As pointed out in Section 2, mass and enstrophy are preserved to machine precision by the HPM method. Figure 5 illustrates the energy conservation property of the HPM method. For this simulation, we chose a coarse discretization of  $J = 128$ , and integrated over an long interval of 30 days using step sizes of  $\Delta t = 432$ s,  $\Delta t = 864$ s, and  $\Delta t = 1728$ . The relative energy errors observed at day 30 were  $2.0859 \times 10^{-8}$ ,  $8.667 \times 10^{-8}$ , and  $1.645 \times 10^{-7}$ , respectively. Note the relatively large errors right at the beginning of the simulation. These are due to the imbalance of the numerical initial data and the rapid subsequent adjustment process.

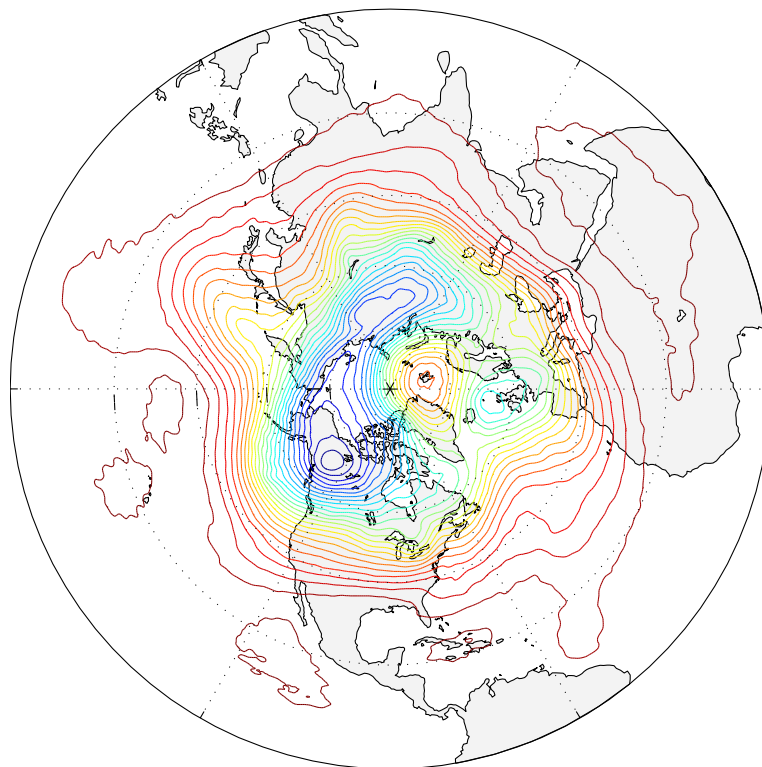


Figure 1: Stereographic projection of 500mb geopotential height field on day 5, Test case 7. Contours by 50m from 9050 (blue) to 10250 (red).

#### REFERENCES

1. Bridges, T.J., Hydon, P., and Reich, S., Vorticity and symplecticity in Lagrangian fluid dynamics, *Proc. Royal Soc. London*, submitted.
2. Côte, J., A Lagrange multiplier approach for the metric terms of semi-Lagrangian models on the sphere, *Q.J.R. Meteorol. Soc.* **114** (1988), 1347–1352
3. Cotter, C.J., and Reich, S., Adiabatic invariance and applications to MD and NWP, *BIT*, submitted.
4. Fornberg, B., A pseudospectral approach for polar and spherical geometries, *SIAM J. Sci. Comput.* **16** (1995), 1071–1081.
5. Frank, J., and Reich, S., Conservation properties of smoothed particle hydrodynamics applied to the shallow water equations, *BIT* **43** (2003), 40–54.
6. Frank, J., Gottwald, G., and Reich, S., A Hamiltonian particle-mesh method for the rotating shallow-water equations, *Lecture Notes in Computational Science and Engineering*, **26**, 131–142, Springer, Heidelberg (2002)
7. Hairer, E., Lubich, C., and Wanner, G., *Geometric Numerical Integration: Structure-Preserving Algorithms for Ordinary Differential Equations*, Springer, Heidelberg (2002)
8. Jakob-Chien, R., Hack, J.J., and Williamson, D.L., Spectral transform solutions to the shallow water test set, *J. Comput. Phys.* **119** (1995), 164–187.
9. Merilees, P.E., The pseudospectral approximation applied to the shallow water equations on the

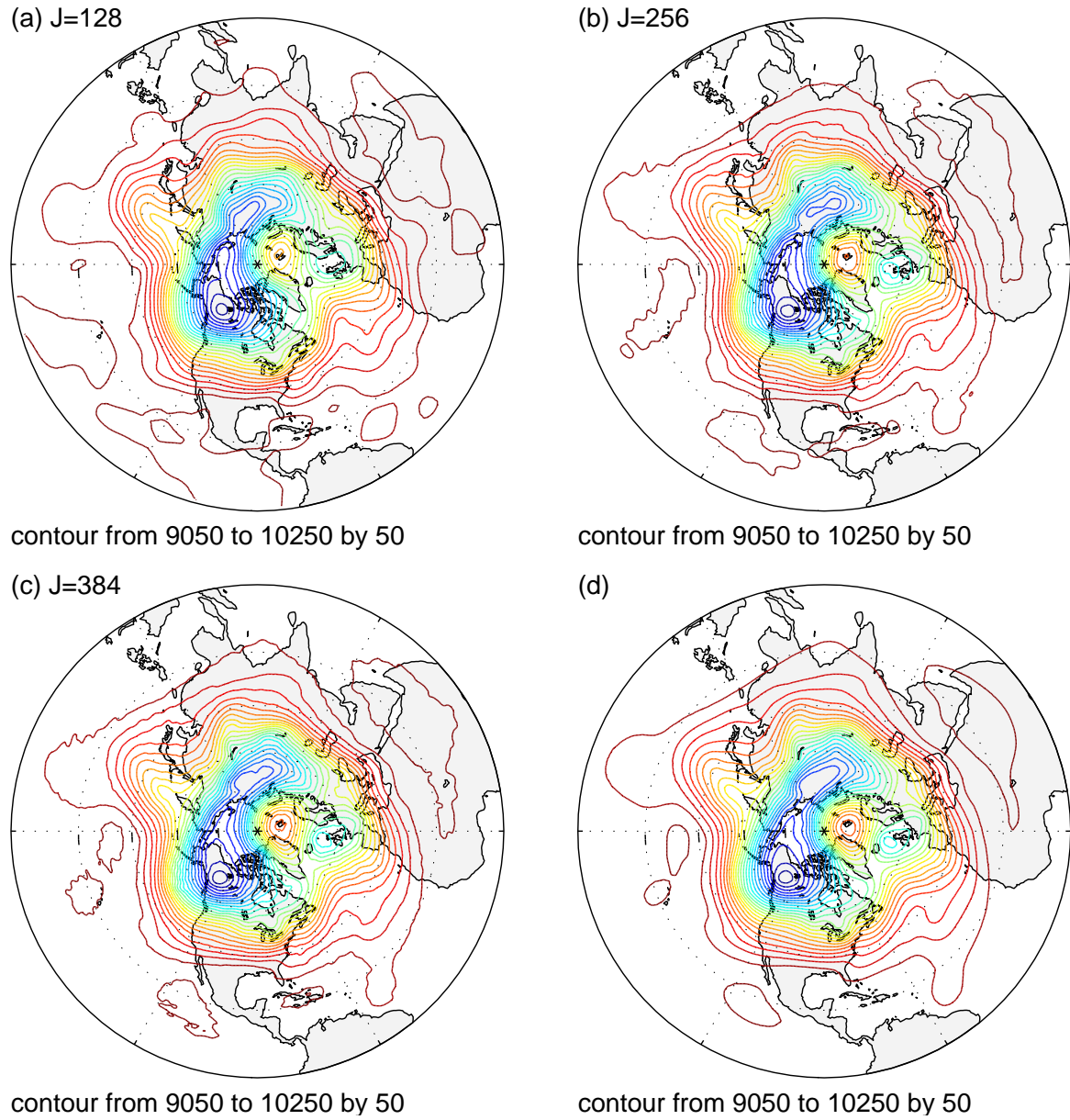
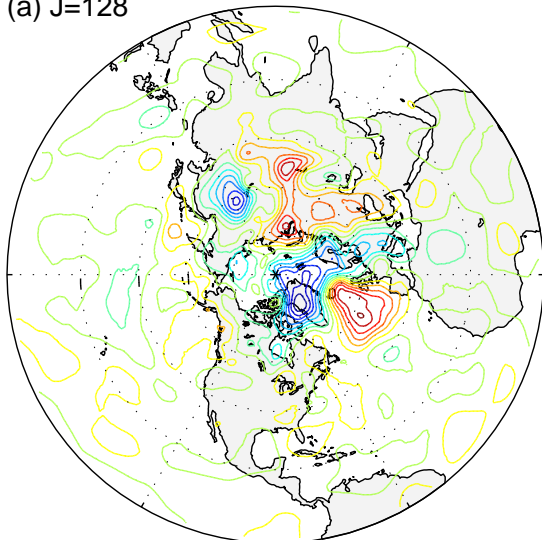
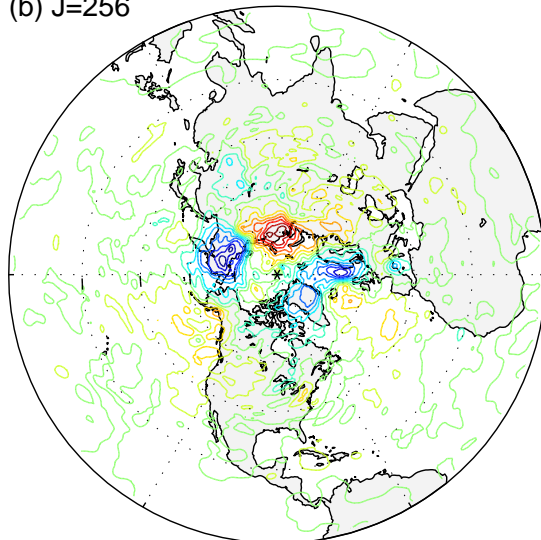
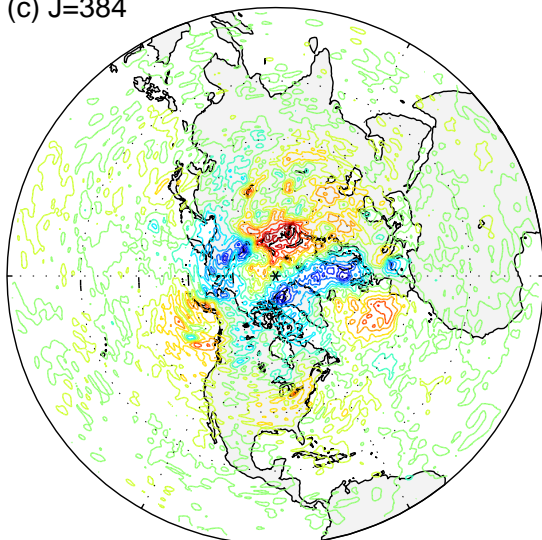


Figure 2: Comparison of Day 5 solution for a)  $J = 128$ , b)  $J = 256$ , c)  $J = 384$ , d) T213 reference solution.

sphere, *Atmosphere* **11** (1973), 13–20.

10. Spatz, W.F., Taylor, M.A., and Swarztrauber, P.N, Fast shallow-water equations solvers in latitude-longitude coordinates, *J. Comput. Phys.* **145** (1998), 432–444.
11. Williamson, D.L., Drake, J.B., Hack, J.J., Jakob, R., and Swarztrauber, P.N., A standard test set for the numerical approximations to the shallow water equations in spherical geometry, *J. Comput. Phys.* **102** (1992), 211–224.

(a)  $J=128$ contour from  $-200$  to  $200$  by  $25$ (b)  $J=256$ contour from  $-100$  to  $100$  by  $12.5$ (c)  $J=384$ contour from  $-50$  to  $50$  by  $6.25$ 

(d)

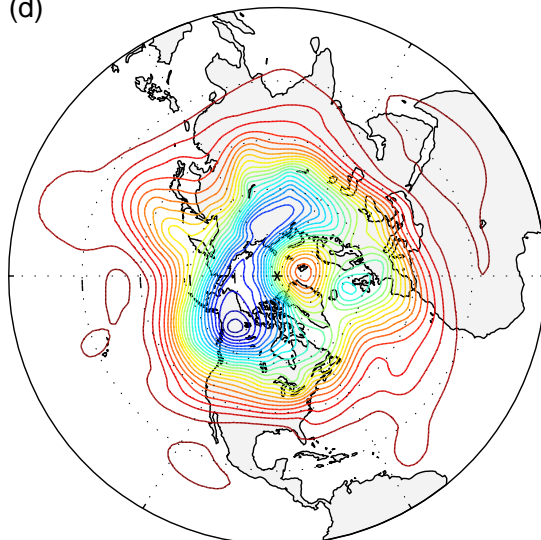
contour from  $9050$  to  $10250$  by  $50$ 

Figure 3: Stereographic projection of error in geopotential on day 5 for a)  $J = 128$ , b)  $J = 256$  and c)  $J = 384$ . The reference solution is reproduced in d).

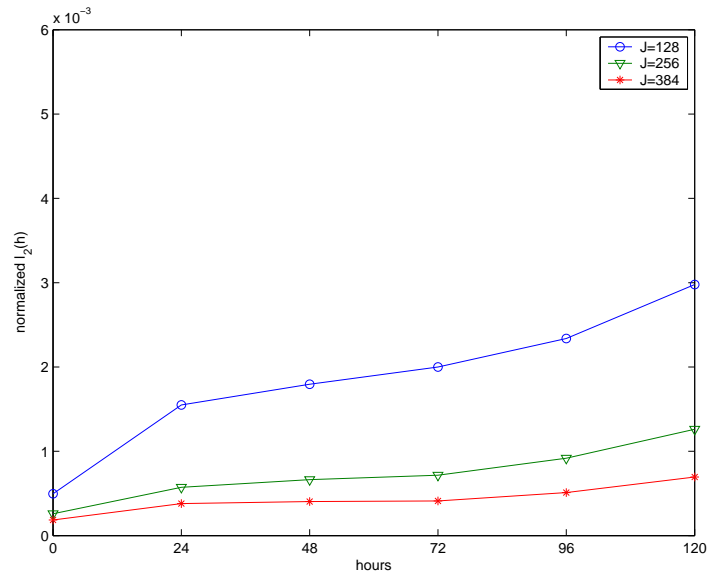


Figure 4: Error growth in the  $\ell_2$ -norm of the geopotential height field.

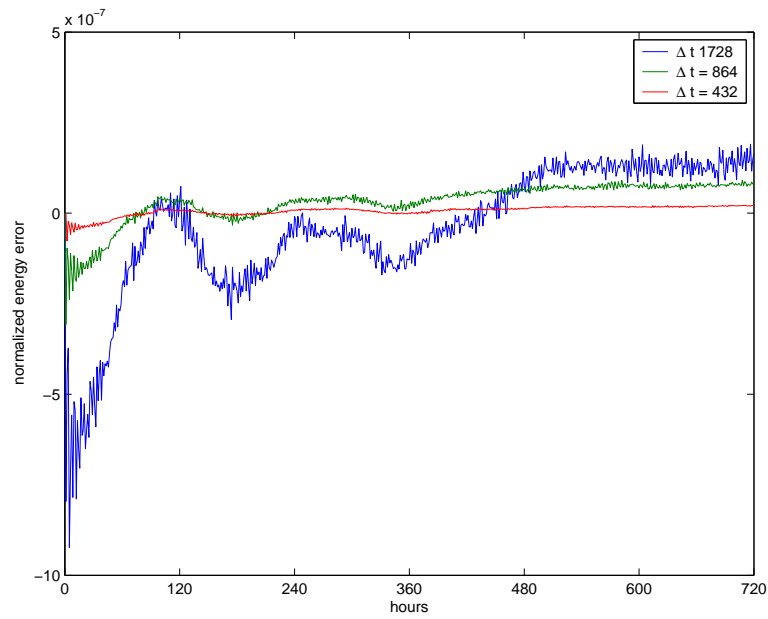


Figure 5: Variation in total energy over a 30 day simulation.